Supporting Information

Kraft lignin solubility and its chemical modification in deep eutectic solvents

Filipe H. B. Sosa[1,2], Dinis O. Abranches[2], André M. da Costa Lopes[2,3*], João A. P. Coutinho[2*], Mariana C. da Costa[1]

[1]Department of Process and Products Design (DDPP) - School of Chemical Engineering (FEQ), University of Campinas (UNICAMP), 13083-852, Campinas, São Paulo, Brazil.

[2]CICECO - Aveiro Institute of Materials, Department of Chemistry, University of Aveiro, 3810-193 Aveiro, Portugal.

[3]CECOLAB - Collaborative Laboratory Towards Circular Economy, R. Nossa Senhora da Conceição, 3405-155 Oliveira do Hospital

*Corresponding author 1: andremcl@ua.pt

*Corresponding author 2: jcoutinho@ua.pt

Number of Pages: 17

Number of Tables: 4

Number of Figures: 6

Table of Contents

1. Chemicals S3

2. Lignin calibration curve S4

3. Kraft lignin solubility in DES S5

4. Shimizu and Matubayasi hydrotropy model S6

5. Lignin characterization S9

5.2. FTIR-ATR S9

5.2. 2D HSQC NMR S11

6. References S15

1. Chemicals

Table S1. Compounds used in this work along with their CAS Number, molecular weight (Mw), purity and supplier.

Compound	CAS Number	Mw (g mol^{-1})	Water content (wt %)	Purity[a] (wt %)	Supplier
Cholinium chloride ([Ch]Cl)	67-48-1	139.62	2.38±0.42	98.0	Acros Organics
Glycerol (GLY)	56-81-5	92.09	0.13±0.04	99.0	Acros Organics
Ethylene glycol (EGLY)	107-21-1	62.07	0.11±0.02	99.0	Fluka
1,3-propanediol (PROP)	504-63-2	76.10	0.09±0.01	98.0	Sigma
1,4-butanediol (BUT)	110-63-4	90.12	0.07±0.01	99.0	Alfa Aesar
1,5-pentanediol (PENT)	111-29-5	104.15	0.05±0.02	97.0	Alfa Aesar
1,6-hexanediol (HEXA)	629-11-8	118.16	0.08±0.01	97.0	Aldrich
L(+)-lactic acid (LacA)	79-33-4	90.08	14.8±0.05	92.0	Riedel de Haen
Oxalic acid (OxaA)	144-62-7	90.03	0.03±0.00	99.5	Merck
DL-malic acid (MaliA)	617-48-1	134.09	0.02±0.00	99.5	Panreac
DL-malonic acid (MaloA)	141-82-2	104.06	0.01±0.00	>98.0	Fluka
Maleic acid (MaleA)	110-16-7	116.07	0.01±0.00	99.0	Panreac

[a]reported by the supplier

2. LIGNIN CALIBRATION CURVE

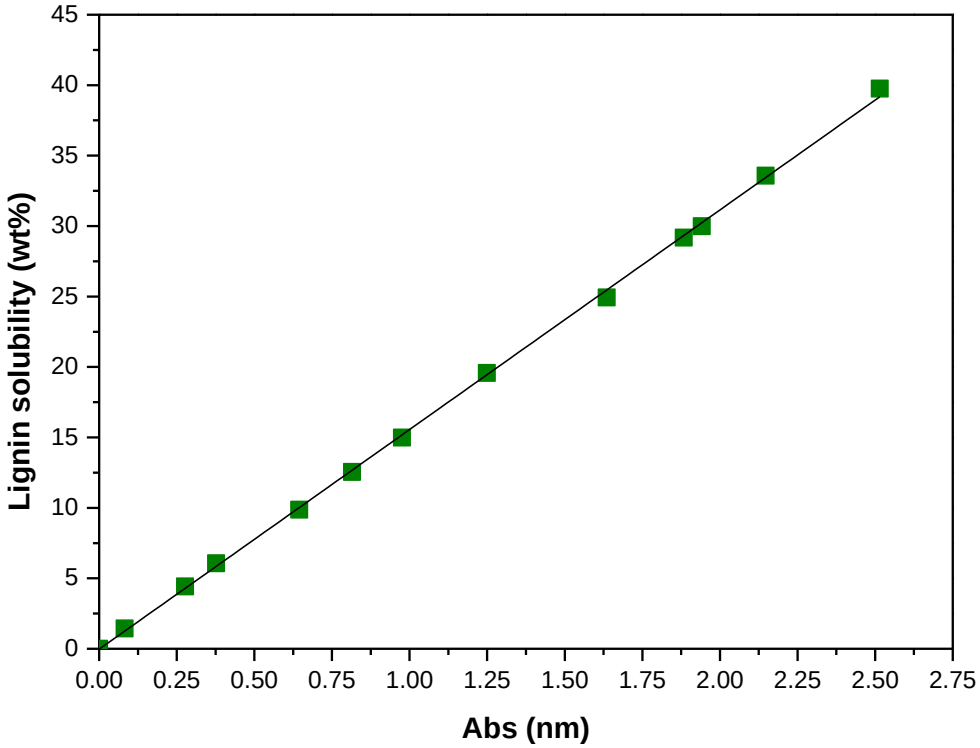

Figure S1. Kraft lignin calibration curve.

3. KRAFT LIGNIN SOLUBILITY IN DES

Table S2. Solubility of Kraft lignin in DES with 5 wt % water content at 313.15 K.

DES	HBA:HBD molar ratio	Lignin solubility (wt%)
	Polyols	
[Ch]Cl:GLY	1:2	28.56±0.89
[Ch]Cl:EGLY	1:2	32.26±0.72
[Ch]Cl:PROP	1:2	25.12±0.58
[Ch]Cl:BUT	1:2	27.61±0.56
[Ch]Cl:PENT	1:2	29.54±0.51
[Ch]Cl:HEXA	1:2	32.99±0.58
	Carboxylic Acids	
[Ch]Cl:OxaA	1:1	23.08±0.30
[Ch]Cl:MaloA	1:1	34.10±0.04
[Ch]Cl:MaliA	1:1	24.74±0.33
[Ch]Cl:MaleA*	1:1	34.97±0.33
[Ch]Cl:OxaA	1:2	23.92±0.47
[Ch]Cl:MaloA	1:2	34.00±0.37
[Ch]Cl:MaliA	1:2	25.24±1.08
	References	
[Ch]Cl:LacA	1:1	28.23±0.24
Water	-	0.15±0.05

*10 wt % water content

4. SHIMIZU AND MATUBAYASI HYDROTROPY MODEL

The Shimizu and Matubayasi[1] model was developed to describe the usual sigmoidal solubility curves found in hydrotropy and also describes information about the interactions between solute and hydrotropic molecules. The model developed by Shimizu and Matubayasi [1] can be described as:

$$\frac{S_L}{S_{L,0}} = \frac{1 + \left(\frac{S_L}{S_{L,0}}\right)_{max} e^{m.ln(x_H)+b}}{1 + e^{m.ln(x_H)+b}}$$

where: $x_H = \frac{M_H}{M_H + M_{water}}$

$x_H = x_{HBD}$ or

$x_H = x_{ChCl}$ or

$x_H = x_{ES} = x_{HBD} + x_{ChCl}$

where S_L is the solubility of lignin in the system (molar fraction of the solute), $S_{L,0}$ is the solubility of lignin in water and x_H is the molar fraction of the hydrotrope, in this case being HBD, or chlorine chloride or the sum of the two in the case of ES. Note that x_H is the molar fraction of the hydrotrope on a solute free base. The term $S_L/S_{L,0}$ represents the relative solubility of lignin in the solution about solubility in pure water. The parameters *m* and *b* represent the molecular interactions between solute and hydrotrope, more specifically, *m* represents the number of hydrotrope molecules in the vicinity of the solute.

After determining the parameters *m* and *b*, it is possible to outline the model curve adjusted to the experimental data.

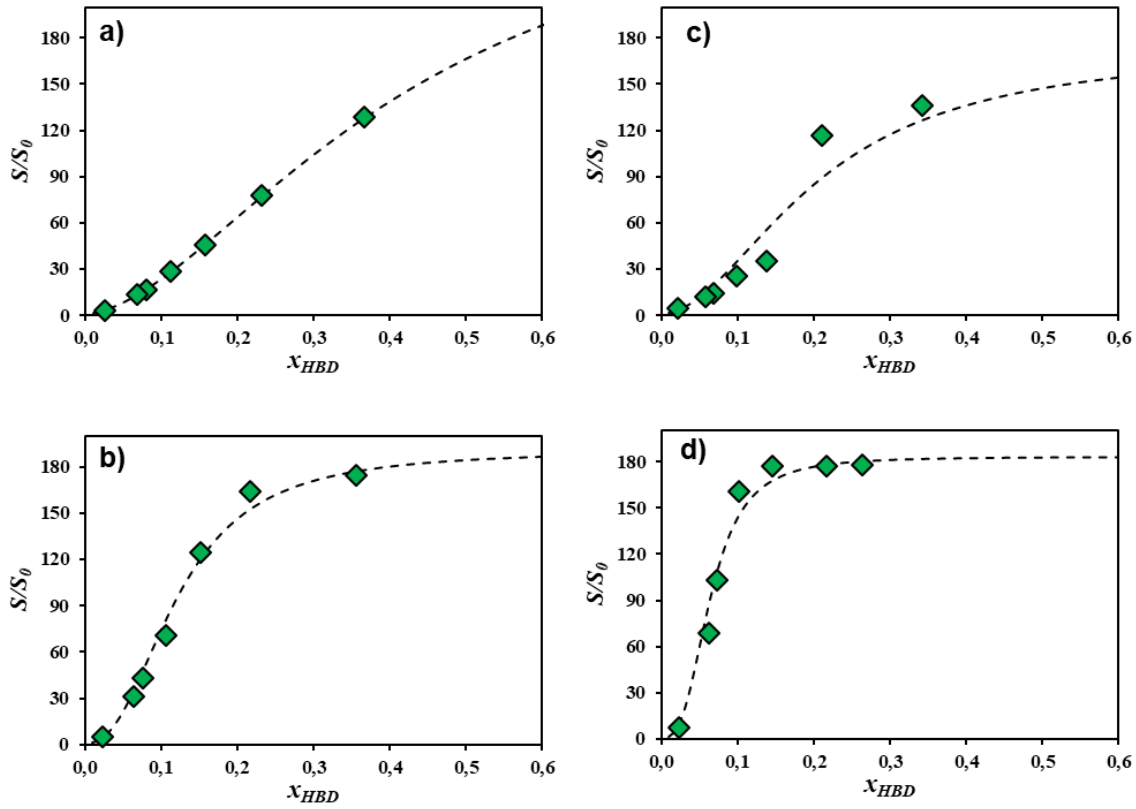

Figure S2. Solubility enhancement of lignin ($S_L/S_{L,0}$) in DES aqueous solutions with the following HBDs: a) OxaA, b) MaloA, c) MaliA, and d) MaleA fitted using the Shimizu and Matubayasi hydrotropy model (- - -).[1]

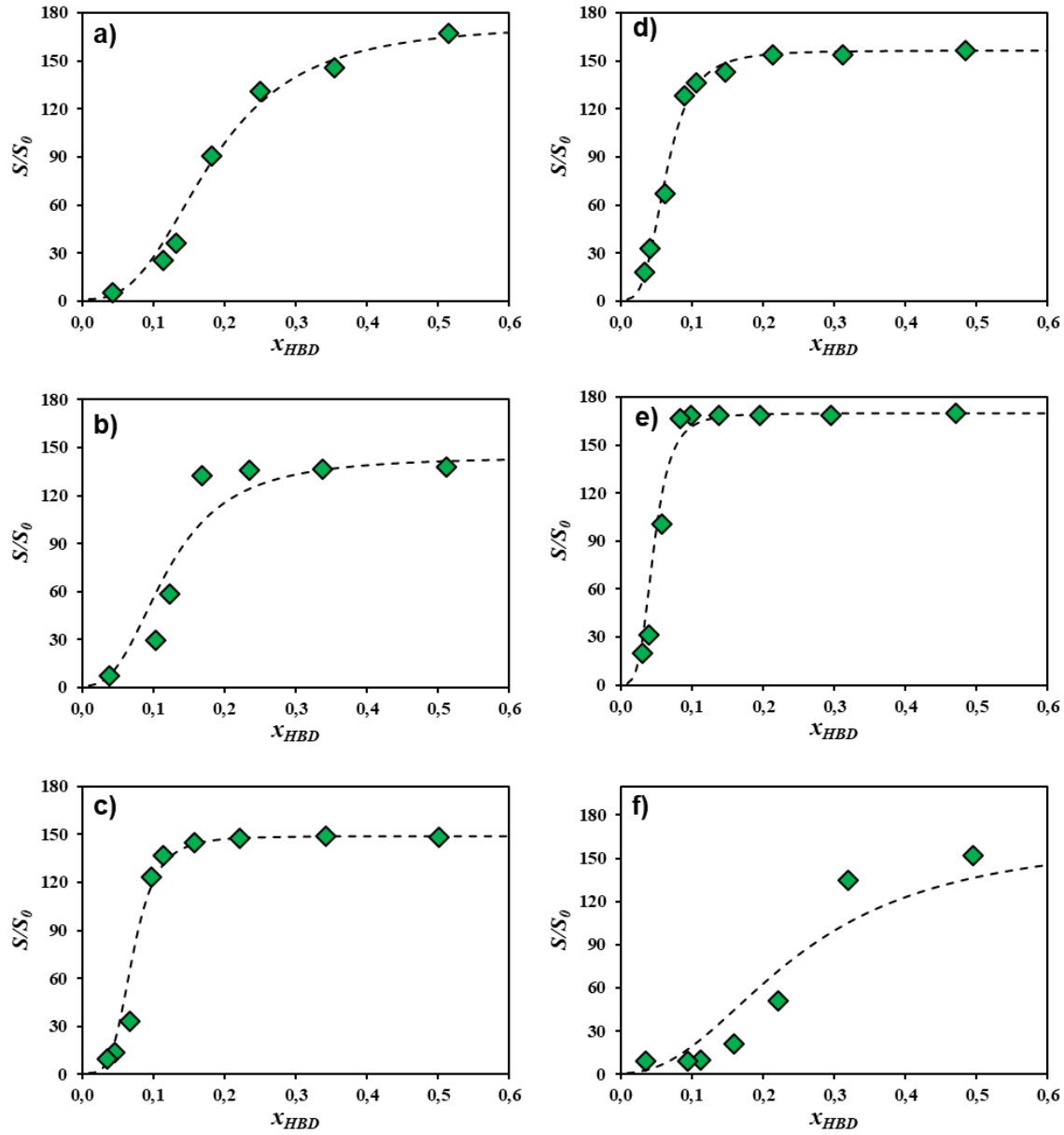

Figure S3. Solubility enhancement of lignin ($S_L/S_{L,0}$) in DES aqueous solutions with the following HBDs: a) ethylene glycol, b) 1,3-propanediol, c) 1,4-butanediol, d) 1,5-pentanediol and e) 1,6-hexanediol and f) glycerol fitted using the Shimizu and Matubayasi hydrotropy model (- - -).[1]

5. LIGNIN CHARACTERIZATION

5.1. FTIR-ATR

Table S3. FTIR vibrational bands/regions and corresponding assignments for Kraft lignin.

Vibrational band/region (cm^{-1})	Assignments
3200-3500	O-H vibrations[2]
2844-2980	Aliphatic C–H and CH2 stretching vibrations[2]
1775-1750	C=O of esters, ketones, aldehydes and acids. (C=O stretching, non conjugated[3]
1731	C=O stretching in xylan, C=O stretching of acetyl or carboxylic acid[4,5]
1700	Unconjugated C=O (ketone, carboxyl or ester stretching)[4,6]
1600-1690	Aromatic skeletal vibration[7–9]
1514	Aromatic skeletal vibration[7–9]
1456	Aromatic skeletal vibration and C-H deformations[7–9]
1425	Aromatic skeletal vibrations combined with C-H in-plane deformation[7–9]
1370-1365	C-H deformation (aliphatic C-H Stretch in CH3, not in OMe; phen. OH[10]
1327-1365	Syringyl unit breathing with C=O stretching and condensed Guaiacyl rings[7–9]
1241	Guaiacyl ring breathing C–O stretch in lignin and for C–O linkage in guiacyl aromatic methoxyl groups[11]
1212	C-C plus C-O plus C=O stretch; Guaiacyl condensed > Guaiacyl etherified[7–9]
1152	C–O–C vibration (Cellulose and hemicellulose)[11]
1109	Contribution of C-H in a plane deformation, C=O stretching of syringyl units and secondary alcohols[7–9]
1040	Aromatic C H in-plane deformation (Guaiacyl > Syringyl) plus C-O deformation in primary alcohols plus C=O stretch (unconjugated) [7–9]
979	C–O valance vibration; aromatic C–H in plane deformation[12]
925	Aromatic C-H out-of-plane[7]
838	Aromatic C-H out-of-plane deformation in Guaiacyl and Syringyl units[13]

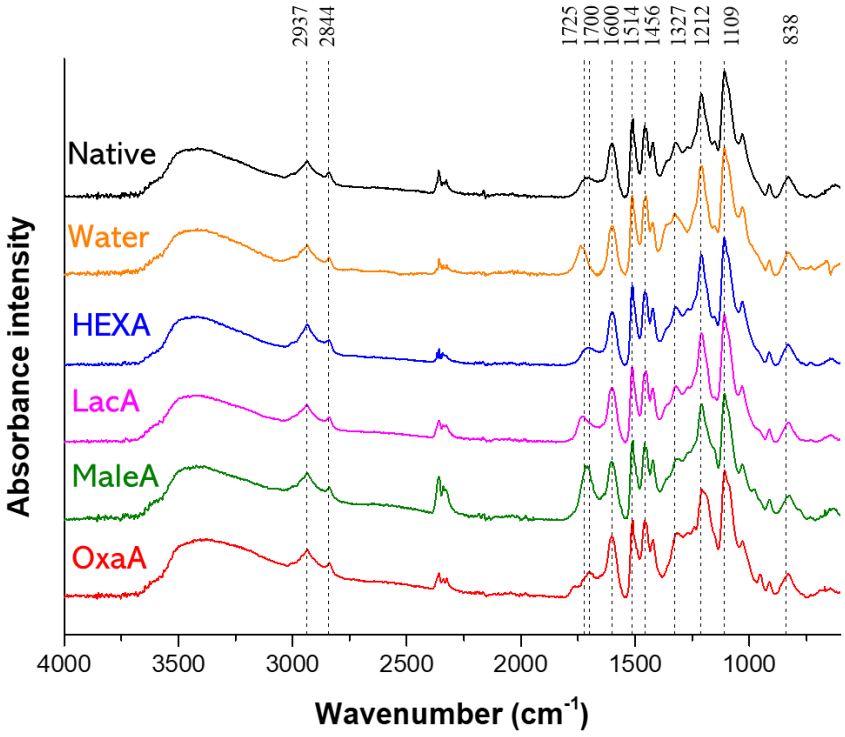

Figure S4. FTIR-ATR spectra of Kraft lignin and recovered lignins from treatments with [Ch]Cl:OxaA, [Ch]Cl:LacA, [Ch]Cl:Hexa, [Ch]Cl:MaleA and water at 393.15 K for 6 h.

5.2. 2D HSQC NMR

The structural analysis of lignin samples was complemented with the 2D HQSC NMR technique to better understand the impact of thermal treatments with DES. The HSQC oxygenated and aromatic regions of the Kraft lignin along with the representation of identified lignin subunits are shown in Figure S5 to suitably address its chemical characterization. The ^{13}C-^{1}H cross signal assignments are described in Table S4 according to data reported in literature. [14–20]

In the oxygenated aliphatic region (δc-δH 35-110/2.5-5.7 ppm), the major lignin subunits, such as alkyl-aryl ether structures (β-O-4), resinols (β-β), phenylcoumaran (β-1), spirodienone (β-5), were identified in Kraft Lignin, while an intense signal at 56.1/3.75 ppm represents the C-H cross assignment of methoxy groups in lignin. On the other hand, cross signals associated with xylan backbone (X) were also found representing a contamination of residual xylan in Kraft lignin, which is a common trait in this technical lignin.[15]

In the aromatic region (δ_C-δ_H 90-160/5.8-9.0 ppm), the cross signals at 104.88/7.07 and 105.22/6.47 ppm refer to the $C_{2,6}$-$H_{2,6}$ correlations in non-oxidized ($S_{2,6}$) and oxidized ($S'_{2,6}$) syringyl type units, respectively. Similar assignments can be made to guaiacyl type units, including non-oxidized at 111.00/6.95 ppm (G_2), 115.00/6.75 ppm (G_5), 119.00/6.75 ppm (G_6); and oxidized at 111.04/7.33 (G'_2) and 120.14/7.24 (G'_6) ppm.[21] The signal range between 122.00-130.00/7.0-8.0 ppm should correspond to α-carbonyl/carboxyl position in syringyl and guaiacyl units[14] as well as to cinnamyl structures with alcohols, aldehydes, and acids as end groups (H).

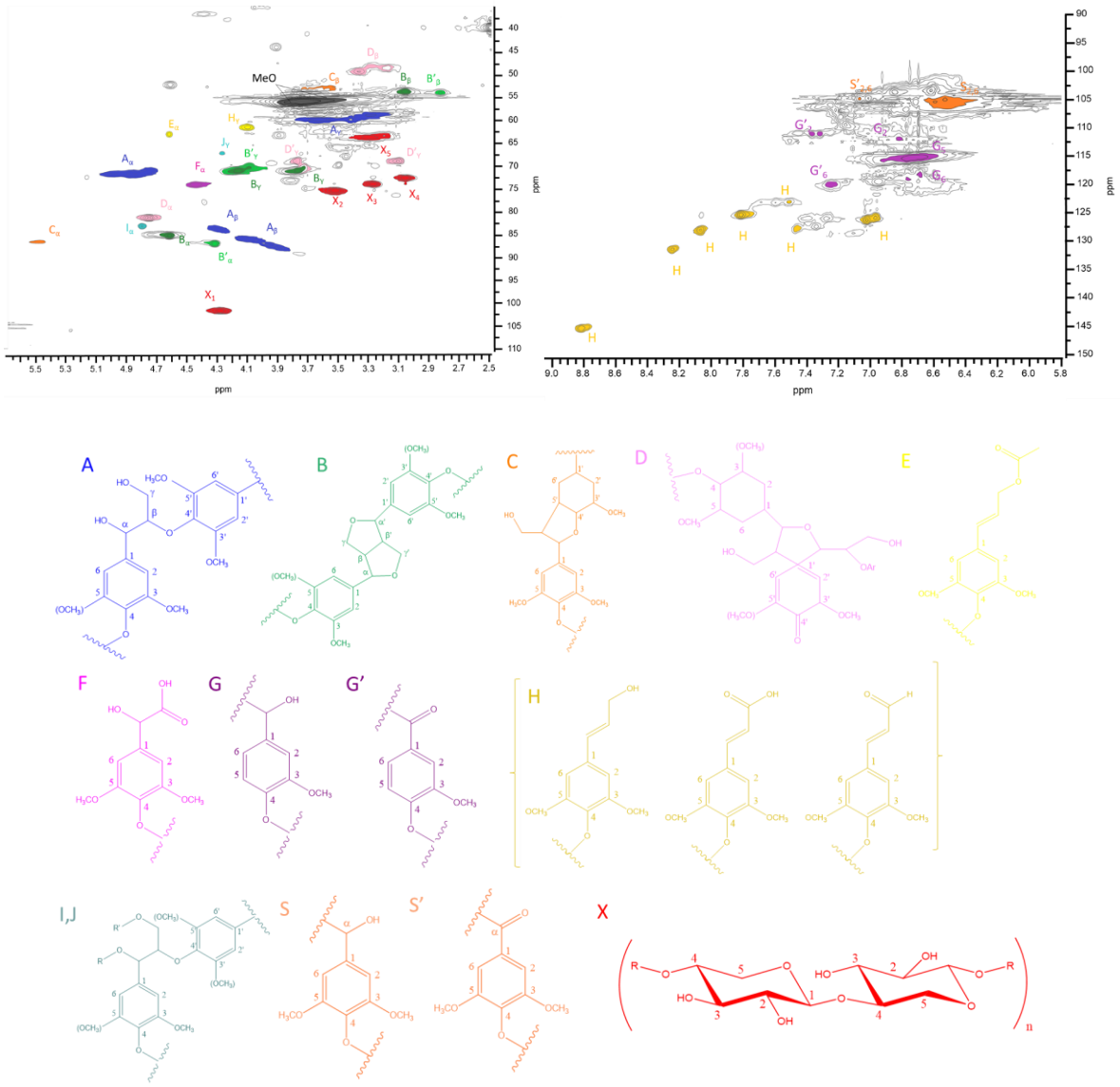

Figure S5. 2D HSQC NMR of Kraft lignin with corresponding ^{13}C-^{1}H cross signal assignments to main lignin subunits: (A) β-O-4' linkages; (B) Resinol (β-β'); (C) Phenylcoumaran (β-5'); (D) Spirodienone (β-1'); (E) cinnamyl acetate end-groups; (F) Ar-CHOH-COOH unit (Cα-Hα); (G) Guaiacyl unit; (G') oxidized Guaiacyl unit with a Cα ketone or carboxyl group; (H) p-hydroxycynnamyl structures (alcohol, aldehyde or carboxylic end groups); (I) β-O-4' substructure Cα etherified to carbohydrate (R, polysaccharide; R', H); (J) β-O-4' substructure Cγ etherified to carbohydrate (R, H; R', polysaccharide); (S2,6) Syringyl unit; (S'2,6) oxidized syringyl unit with a Cα ketone (phenolic); (X) Xylan.

Table S4. Assignments of Kraft lignin C-H correlation signals in the HSQC spectra.

Labels	δC	δH	Assignment
Dβ	49.61	3.39	C_β-H_β in β-1′ spirodienone substructures (D)
Bβ	53.50	3.07	C_β-H_β in resinol substructures (B)
Cβ	53.71	3.46	C_β-H_β in β-5 phenylcoumaran
B′β	54.20	2.82	C_β-H_β in epiresinol substructures (B)
MeO	56.06	3.75	C-H in methoxyls
Aγ	59.00	3.2	C_γ-H_γ in β-O-4′ substructures (A)
Aγ	59.87	3.71	C_γ-H_γ in β-O-4′ substructures (A)
Hγ	61.59	4.11	C_γ-H_γ in p-hydroxycynnamyl alcohol
Eα	63.16	4.64	C_α-H_α in p-hydroxycinnamyl alcohol
Cγ	63.26	3.89	C_γ-H_γ in β-5 phenylcoumaran
X5	63.63	3.28	C_5-H_5 in xylan
Jγ	66.88	4.28	C_γ-H_γ in β-O-4′ Cα- etherified with carbohydrate
Dγ′	68.89	3.79	C_γ-H_γ in β-1′ spirodienone substructures (D)
Dγ′	68.92	3.13	C_γ-H_γ in β-1′ spirodienone substructures (D)
B′β	70.56	4.09	C_β-H_β in epiresinol substructures (B)
Bγ	71.07	3.79	C_γ-H_γ in resinol substructures (B)
Bγ	71.14	4.2	C_γ-H_γ in resinol substructures (B)
Aα	71.62	4.91	C_α-H_α in β-O-4′ substructures (A)
X4	72.85	3.06	C_4-H_4 in xylan
Fα	74.18	4.43	C_α-H_α in Ar-CHOH-COOH unit
X3	74.28	3.28	C_3-H_3 in xylan
X2	75.84	3.53	C_2-H_2 in xylan
B′α	81.36	4.78	C_α-H_α in epiresinol substructures (B)
Cα	82.92	5.51	Cα-Hα in β-5 phenylcoumaran
Iα	83.41	4.83	Cα-Hα in β-O-4′ Cα- etherified with carbohydrate
Aβ	83.96	4.31	(G) CβHβ in β-O-4′ linked to G units
Bα	85.3	4.67	C_α-H_α in resinol substructures (B)
Dβ′	86.89	4.44	C_β -H_β in β-1′ spirodienone substructures (D)
B′α	87.22	4.33	C_α-H_α in epiresinol substructures (B)
Aβ	87.23	3.69	(S) C_β-H_β in β-O-4′ linked to S units
X1	101.8	4.29	C_1-H_1 in xylan
S′2.6	104.88	7.07	$C_{2.6}$ - $H_{2.6}$ in oxidized Syringyl units (S′)

S2.6	105.22	6.47	$C_{2.6}$ - $H_{2.6}$ in Syringyl units (S)
G2	111.00	6.95	C_2-H_2 in Guaiacyl units (G)
G2’	111.04	7.33	C_2-H_2 in oxidized Guaiacyl units (G)
G5	115.00	6.75	C_5-H_5 in Guaiacyl units (G)
G6	119.00	6.75	C_6-H_6 in Guaiacyl units (G)
G6’	120.14	7.24	C_6-H_6 in oxidized Guaiacyl units (G)
H	122.98	7.56	Cynnamyl alcohols. aldehydes or acids (end groups)
H	125.53	7.79	Cynnamyl alcohols. aldehydes or acids (end groups)
H	126.16	4.00	Cynnamyl alcohols. aldehydes or acids (end groups)
H	127.01	7.35	Cynnamyl alcohols. aldehydes or acids (end groups)
H	128.42	8.09	Cynnamyl alcohols. aldehydes or acids (end groups)
H	131.29	8.23	Cynnamyl alcohols. aldehydes or acids (end groups)
H	145.73	8.8	Cynnamyl alcohols. aldehydes or acids (end groups)

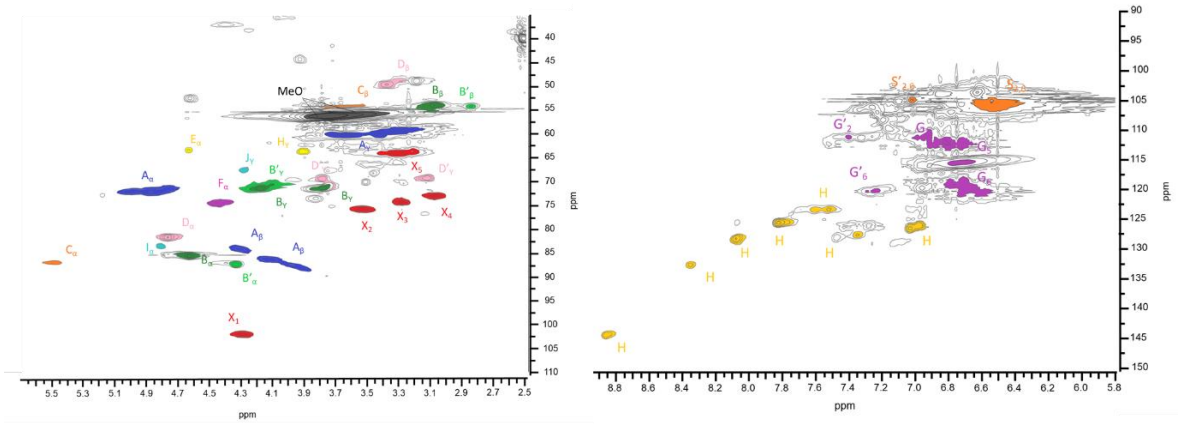

Figure S6. 2D HSQC NMR of recovered lignins from thermal treatment with water at 393.15 K for 6 h.

6. REFERENCES

(1) Shimizu, S.; Matubayasi, N. The Origin of Cooperative Solubilisation by Hydrotropes. *Phys. Chem. Chem. Phys.* **2016**, *18* (36), 25621–25628. DOI 10.1039/c6cp04823d.

(2) Nevrez, L. A. M.; Casarrubias, L. B.; Celzard, A.; Fierro, V.; Mũoz, V. T.; Davila, A. C.; Lubian, J. R. T.; Snchez, G. G. Biopolymer-Based Nanocomposites: Effect of Lignin Acetylation in Cellulose Triacetate Films. *Sci. Technol. Adv. Mater.* **2011**, *12* (4), 045006. DOI 10.1088/1468-6996/12/4/045006.

(3) Rodrigues, J.; Faix, O.; Pereira, H. Determination of Lignin Content of Eucalyptus Globulus Wood Using FTIR Spectroscopy. *Holzforschung* **1998**, *52* (1), 46–50. DOI 10.1515/hfsg.1998.52.1.46.

(4) Chow, S. Z. Infrared Spectral Characteristics and Surface Inactivation of Wood at High Temperatures. *Wood Sci. Technol.* **1971**, *5* (1), 27–39. DOI 10.1007/BF00363118.

(5) Fackler, K.; Stevanic, J. S.; Ters, T.; Hinterstoisser, B.; Schwanninger, M.; Salmén, L. Localisation and Characterisation of Incipient Brown-Rot Decay within Spruce Wood Cell Walls Using FT-IR Imaging Microscopy. *Enzyme Microb. Technol.* **2010**, *47* (6), 257–267. DOI 10.1016/j.enzmictec.2010.07.009.

(6) Cachet, N.; Camy, S.; Benjelloun-Mlayah, B.; Condoret, J. S.; Delmas, M. Esterification of Organosolv Lignin under Supercritical Conditions. *Ind. Crops Prod.* **2014**, *58*, 287–297. DOI 10.1016/j.indcrop.2014.03.039.

(7) Prado, R.; Erdocia, X.; De Gregorio, G. F.; Labidi, J.; Welton, T. Willow Lignin Oxidation and Depolymerization under Low Cost Ionic Liquid. *ACS Sustain. Chem. Eng.* **2016**, *4* (10), 5277–5288. DOI 10.1021/acssuschemeng.6b00642.

(8) García, A.; Erdocia, X.; González Alriols, M.; Labidi, J. Effect of Ultrasound Treatment on the Physicochemical Properties of Alkaline Lignin. *Chem. Eng. Process. Process Intensif.* **2012**, *62*, 150–158. DOI 10.1016/j.cep.2012.07.011.

(9) Sun, S. N.; Li, M. F.; Yuan, T. Q.; Xu, F.; Sun, R. C. Sequential Extractions and Structural

Characterization of Lignin with Ethanol and Alkali from Bamboo (Neosinocalamus Affinis). *Ind. Crops Prod.* **2012**, *37* (1), 51–60. DOI 10.1016/j.indcrop.2011.11.033.

(10) Passoni, V.; Scarica, C.; Levi, M.; Turri, S.; Griffini, G. Fractionation of Industrial Softwood Kraft Lignin: Solvent Selection as a Tool for Tailored Material Properties. *ACS Sustain. Chem. Eng.* **2016**, *4* (4), 2232–2242. DOI 10.1021/acssuschemeng.5b01722.

(11) Pandey, K. K.; Pitman, A. J. FTIR Studies of the Changes in Wood Chemistry Following Decay by Brown-Rot and White-Rot Fungi. *Int. Biodeterior. Biodegrad.* **2003**, *52* (3), 151–160. DOI 10.1016/S0964-8305(03)00052-0.

(12) Schwanninger, M.; Hinterstoisser, B.; Gierlinger, N.; Wimmer, R.; Hanger, J. Application of Fourier Transform near Infrared Spectroscopy (FT-NIR) to Thermally Modified Wood. *Holz als Roh - und Werkst.* **2004**, *62* (6), 483–485. DOI 10.1007/s00107-004-0520-z.

(13) Gordobil, O.; Delucis, R.; Egüés, I.; Labidi, J. Kraft Lignin as Filler in PLA to Improve Ductility and Thermal Properties. *Ind. Crops Prod.* **2015**, *72*, 46–53. DOI 10.1016/j.indcrop.2015.01.055.

(14) Balakshin, M. Y.; Capanema, E. A.; Chen, C. L.; Gracz, H. S. Elucidation of the Structures of Residual and Dissolved Pine Kraft Lignins Using an HMQC NMR Technique. *J. Agric. Food Chem.* **2003**, *51* (21), 6116–6127. DOI 10.1021/jf034372d.

(15) Liitiä, T. M.; Maunu, S. L.; Hortling, B.; Toikka, M.; Kilpeläinen, I. Analysis of Technical Lignins by Two- and Three-Dimensional NMR Spectroscopy. *J. Agric. Food Chem.* **2003**, *51* (8), 2136–2143. DOI 10.1021/jf0204349.

(16) Rencoret, J.; Marques, G.; Gutiérrez, A.; Nieto, L.; Jiménez-Barbero, J.; Martínez, Á. T.; del Río, J. C. Isolation and Structural Characterization of the Milled-Wood Lignin from Paulownia Fortunei Wood. *Ind. Crops Prod.* **2009**, *30* (1), 137–143. DOI 10.1016/j.indcrop.2009.03.004.

(17) Balakshin, M.; Capanema, E.; Chen, C. L.; Gratzl, J.; Kirkman, A.; Gracz, H. Biobleaching of Pulp with Dioxygen in the Laccase-Mediator System - Reaction Mechanisms for

Degradation of Residual Lignin. *J. Mol. Catal. - B Enzym.* **2001**, *13* (1–3), 1–16. DOI 10.1016/S1381-1177(00)00225-3.

(18) Chen, Z.; Bai, X.; Lusi, A.; Wan, C. High-Solid Lignocellulose Processing Enabled by Natural Deep Eutectic Solvent for Lignin Extraction and Industrially Relevant Production of Renewable Chemicals. *ACS Sustain. Chem. Eng.* **2018**, *6* (9), 12205–12216. DOI 10.1021/acssuschemeng.8b02541.

(19) Chen, Z.; Reznicek, W. D.; Wan, C. Aqueous Choline Chloride: A Novel Solvent for Switchgrass Fractionation and Subsequent Hemicellulose Conversion into Furfural. *ACS Sustain. Chem. Eng.* **2018**, *6* (5), 6910–6919. DOI 10.1021/acssuschemeng.8b00728.

(20) Rencoret, J.; Gutiérrez, A.; Nieto, L.; Jiménez-Barbero, J.; Faulds, C. B.; Kim, H.; Ralph, J.; Martínez, Á. T.; del Río, J. C. Lignin Composition and Structure in Young versus Adult Eucalyptus Globulus Plants. *Plant Physiol.* **2011**, *155* (2), 667–682. DOI 10.1104/pp.110.167254.

(21) Kim, H.; Ralph, J. Solution-State 2D NMR of Ball-Milled Plant Cell Wall Gels in DMSO-d 6/Pyridine-D5. *Org. Biomol. Chem.* **2010**, *8* (3), 576–591. DOI 10.1039/b916070a.